HHS Public Access
Author manuscript
Eur J Nucl Med Mol Imaging. Author manuscript; available in PMC 2021 June 11.

Published in final edited form as:
Eur J Nucl Med Mol Imaging. 2016 September ; 43(10): 1784–1791. doi:10.1007/s00259-016-3357-x.

PET/CT comparing ^{68}Ga-DOTATATE and other radiopharmaceuticals and in comparison with CT/MRI for the localization of sporadic metastatic pheochromocytoma and paraganglioma

Ingo Janssen[1,2], **Clara C. Chen**[3], **Corina M. Millo**[4], **Alexander Ling**[5], **David Taieb**[6], **Frank I. Lin**[7], **Karen T. Adams**[1], **Katherine I. Wolf**[1], **Peter Herscovitch**[4], **Antonio T. Fojo**[8], **Inga Buchmann**[2], **Electron Kebebew**[9], **Karel Pacak**[1]

[1]Program in Adult and Reproductive Endocrinology, Eunice Kennedy Shriver National Institute of Child Health and Human Development, National Institutes of Health, Building 10, CRC, Room 1E-3140, 10 Center Drive MSC-1109, Bethesda, MD 20892, USA

[2]Department of Radiology and Nuclear Medicine, Section of Nuclear Medicine, University Hospital Schleswig Holstein, Campus Lübeck, Ratzeburger Allee 160, 23538 Lübeck, Germany

[3]Nuclear Medicine Division, Radiology & Imaging Sciences, National Institutes of Health Clinical Center, Bethesda, MD 20892, USA

[4]Positron Emission Tomography Department, National Institutes of Health Clinical Center, National Institutes of Health, Bethesda, MD 20892, USA

[5]Radiology and Imaging Sciences, National Institutes of Health Clinical Center, Bethesda, MD 20892, USA

[6]Department of Nuclear Medicine, La Timone University Hospital, CERIMED, Aix-Marseille University, Marseille, France

[7]Cancer Imaging Program, National Cancer Institute, National Institutes of Health, Bethesda, MD 20892, USA

[8]Endocrine Oncology Branch, National Cancer Institute, Bethesda, MD 20892, USA

[9]Center for Cancer Research, National Cancer Institute, Bethesda, MD 20892, USA

Abstract

Purpose—Pheochromocytomas/paragangliomas (PPGLs) and their metastases are tumors that predominantly express somatostatin receptor 2 (SSR2). ^{68}Ga-DOTA(0)-Tyr(3)-octreotate (^{68}Ga-DOTATATE) is a PET radiopharmaceutical with both high and selective affinity for SSRs. The

---

Karel Pacak, karel@mail.nih.gov.

Conflicts of interest None.

Ethical approval All procedures performed in studies involving human participants were in accordance with the ethical standards of the institutional and/or national research committee and with the principles of the 1964 Declaration of Helsinki and its later amendments or comparable ethical standards.

Informed consent Informed consent was obtained from all individual participants included in the study.

purpose of this study was to evaluate the utility of ^{68}Ga-DOTATATE in comparison with other specific and nonspecific radiopharmaceuticals recommended in the current guidelines for the localization of metastatic sporadic PPGL by PET/CT.

Methods—This prospective study included 22 patients (15 men, 7 women; aged 50.0 ± 13.9 years) with confirmed metastatic PPGL, a negative family history for PPGL, and negative genetic testing, who underwent ^{68}Ga-DOTATATE, ^{18}F-fluoro-2-deoxy-D-glucose (^{18}F-FDG) PET/CT, and CT/MRI. Only 12 patients underwent an additional ^{18}F-fluorodihydroxyphenylalanine (^{18}F-FDOPA) PET/CT scan and only 11 patients underwent an additional ^{18}F-fluorodopamine (^{18}F-FDA) PET/CT scan. The rates of detection of metastatic lesions were compared among all the imaging studies. A composite of all functional and anatomical imaging studies served as the imaging comparator.

Results—^{68}Ga-DOTATATE PET/CT showed a lesion-based detection rate of 97.6 % (95 % confidence interval, CI, 95.8 – 98.7 %). ^{18}F-FDG PET/CT, ^{18}F-FDOPA PET/CT, ^{18}F-FDA PET/CT, and CT/MRI showed detection rates of 49.2 % (CI 44.5 – 53.6 %; $p < 0.01$), 74.8 % (CI 69.0 – 79.9 %); $p < 0.01$), 77.7 % (CI 71.5 – 82.8 %; $p < 0.01$), and 81.6 % (CI 77.8 – 84.8 %; $p < 0.01$), respectively.

Conclusion—The results of this study demonstrate the superiority of ^{68}Ga-DOTATATE PET/CT in the localization of sporadic metastatic PPGLs compared to all other functional and anatomical imaging modalities, and suggest modification of future guidelines towards this new imaging modality.

Keywords

^{68}Ga-DOTATATE; ^{18}F-FDG; Pheochromocytoma; Paraganglioma; Metastatic

Introduction

Pheochromocytomas/paragangliomas (PPGLs) are tumors derived from sympathetic tissue in adrenal or extraadrenal abdominal locations or from parasympathetic tissue in the thorax, head, or neck [1]. More than 35 % of PPGLs are hereditary [2], and patients with hereditary tumors that have underlying succinate dehydrogenase subunit B (*SDHB*) mutations are at the highest risk of developing metastatic disease [3]. However, 50 % of metastatic PPGLs occur in patients with sporadic disease, in whom no mutation can be found [4].

PPGLs overexpress somatostatin receptors (SSR), especially SSR2 [5], and the recently developed ^{68}Ga-labeled DOTA peptides have been shown to be far superior to ^{111}In-DTPA-octreotide (Octreoscan®) for the detection of neuroendocrine tumor (NET) lesions [6]. A number of promising studies utilizing ^{68}Ga-DOTA peptide imaging in mostly mixed populations of patients with PPGL, including patients with sympathetic and parasympathetic PPGLs, have recently been published [7-12], including a study by our group which focused exclusively on *SDHB* mutation-related metastatic PPGLs [13]. However, a prospective evaluation of ^{68}Ga-DOTA(0)-Tyr(3)-octreotate (^{68}Ga-DOTATATE) focusing exclusively on patients with sporadic metastatic PPGLs has not so far been performed.

Since proper staging and early detection of metastatic disease are key factors in choosing an appropriate treatment plan, in follow-up, and in predicting outcome in these patients [14], the primary goal of this study was to evaluate the diagnostic utility of ^{68}Ga-DOTATATE PET/CT in this patient group. Secondarily, since *SDHB* mutation-related PPGLs have different functional imaging signatures compared with sporadic metastatic PPGLs [15] and have recently been shown to have higher SSR expression than sporadic tumors [16], it was also of great interest to determine whether and/or how these differences would affect the relative diagnostic performance of ^{68}Ga-DOTATATE in this patient group compared to metastatic PPGLs with underlying *SDHB* mutation.

Our third goal was to evaluate these patients for their potential eligibility for peptide receptor radionuclide therapy (PRRT), since DOTA peptides can also be labeled with therapeutic β-emitters such as ^{177}Lu and ^{90}Y. Treatment options are otherwise very limited in patients with metastatic PPGLs, since they often show only faint or even absent $^{123/131}$I-metaiodobenzylguanidine (MIBG) uptake [17, 18] and are therefore not eligible for ^{131}I-MIBG treatment. In those who show relevant $^{123/131}$I-MIBG uptake, the treatment response is only about 30 % [19]. Furthermore, the use of chemotherapy with cyclophosphamide, vincristine and dacarbazine (CVD; response rate about 37 % [20]) is reserved for patients with rapidly growing tumors or extensive organ tumor burden (especially in the liver) and is limited by treatment-related toxicity.

In this study, we compared ^{68}Ga-DOTATATE PET/CT with ^{18}F-fluoro-2-deoxy-D-glucose (^{18}F-FDG) PET/CT (^{18}F-FDG being the currently best available and recommended radiopharmaceutical for metastatic PPGL imaging [21]) and CT/MRI. Additional comparisons with ^{18}F-fluorodihydroxyphenylalanine (^{18}F-FDOPA) and ^{18}F-fluorodopamine (^{18}F-FDA) were possible in only 12 and 11 patients, respectively. Because histological proof was not feasible in many metastatic lesions, the composite of both anatomical and all functional imaging tests was used as the imaging comparator as described previously [13] and as supported by several investigators [22].

Materials and methods

Patients

Between January 2014 and July 2015, 22 consecutive patients (15 men, 7 women; mean age 50.0 ± 13.9 years) with apparent sporadic metastatic PPGL were prospectively evaluated at the Eunice Kennedy Shriver National Institute of Child Health and Human Development (NICHD) at the National Institutes of Health (NIH). All patients had proven PPGL based on histopathology. All patients had a negative family history of PPGL and underwent genetic testing with negative results (detailed results are provided in Table 1). The study protocol was approved by the institutional review board of the Eunice Kennedy Shriver NICHD (protocol 00-CH-0093) and the NIH Radiation Safety Committee. All patients provided written informed consent for all clinical, genetic, biochemical, and imaging studies for their PPGLs.The mean age of the patients at diagnosis of the primary PPGL was 41.2 ± 15.6 years. Patient characteristics are summarized in Table 1.

Imaging techniques

CT and MRI scans of the neck, chest, abdomen, and pelvis were performed as previously described [13]. All 22 patients underwent ^{68}Ga-DOTATATE and ^{18}F-FDG PET/CT, and CT/MRI. In addition, 12 patients also underwent ^{18}F-FDOPA PET/CT and 11 underwent ^{18}F-FDA PET/CT. All imaging studies were performed within a median of 8.5 days.

PET/CT scans from the upper thighs to the skull were performed 60 min, 60 min, 30 min, and approximately 8 min after intravenous injection of ^{68}Ga-DOTATATE, ^{18}F-FDG, ^{18}F-FDOPA, and ^{18}F-FDA at mean administered activities of 191.4±8.3 MBq, 316.5±59.4 MBq, 466.3±13.0 MBq, and 39.3 ± 0.7 MBq, respectively. Carbidopa (200 mg) was administered orally 60 min before each ^{18}F-FDOPA scan [23]. All PET/CT scans were performed on a Siemens Biograph-mCT 64 scanner and a Biograph-mCT 128 PET/CT scanner (Siemens Medical Solutions). PET images were reconstructed using an iterative algorithm provided by the manufacturer, also utilizing point spread function and time of flight. Low-dose CT scans for attenuation correction and anatomical coregistration were performed without administration of contrast agent and were used for anatomical localization.

Analysis of data

^{68}Ga-DOTATATE PET/CT studies were read independently by two nuclear medicine physicians blinded to all imaging and clinical data except the diagnosis, sex, and age of the patient. Maximal standardized uptake values (SUV_{max}) were determined and focal areas of abnormal uptake with a higher SUV_{max} than surrounding tissue were considered as lesions. In all other imaging studies, physicians were blinded to ^{68}Ga-DOTATATE PET/CT and clinical data except for diagnosis, sex and age of the patient, and previous imaging studies. The composite of anatomical and all performed functional imaging tests was considered the imaging comparator. A positive result with at least two different functional imaging modalities or at least one functional imaging study and CT/MRI was counted as true disease, whereas a lesion detected only on CT/MRI or only with one functional imaging modality, while negative on all other used imaging tests, was considered a false-positive imaging result. This approach is consistent with our previously used imaging comparator [13] and is consistent with the recommendation of Hofman and Hicks for studies involving patient cohorts in whom histological proof is neither feasible nor ethical [22].

For regional analysis, adrenal glands, liver, abdominal/pelvic compartments (excluding adrenal glands and liver), lungs, mediastinum, and bone were analyzed separately. A patient or region was considered positive regardless of the number of positive findings. Per patient, per region, and per lesion analyses were performed. If the number of lesions in a region exceeded 15, the count was truncated at 15. Soft tissue lesions in the neck (due to their parasympathetic origin) as well as skull and extremity lesions, for which anatomical correlation and/or correlation on ^{18}F-FDG imaging was not available, were excluded from evaluation.

Statistics

Results are given as means with 95 % confidence intervals (CIs) unless stated otherwise. For statistical analysis, the McNemar test was used to compare detection rates between ^{68}Ga-

DOTATATE PET/CT and the other imaging modalities. Two-sided p values <0.05 were considered significant.

Results

On ^{68}Ga-DOTATATE PET/CT, 450 out of 461 lesions (97.6 %, CI 95.8 – 98.7 %) with a mean SUV_{max} of 51.7 ± 49.2 were identified compared with the defined imaging comparator. ^{18}F-FDG, ^{18}F-FDOPA and ^{18}F-FDA PET/CT, and CT/MRI showed detection rates of 49.2 % (CI 44.5 – 53.6 %; $p < 0.01$), 74.8 % (CI 69.0 – 79.9 %; $p < 0.01$), 77.7 % (CI 71.5 – 82.8 %; $p < 0.01$), and 81.6 % (CI 77.8 – 84.8 %; $p < 0.01$), respectively. Significantly more lesions were identified on ^{68}Ga-DOTATATE PET/CT compared with all other functional imaging modalities and with CT/MRI (two-sided $p < 0.01$ for each imaging modality compared with ^{68}Ga-DOTATATE PET/CT). Lesion-based findings are summarized in Tables 2 and 3. Metastatic lesions were found in the mediastinum, lungs, liver, abdominal/ pelvic compartment, and bones. Those in the mediastinum and abdominal/pelvic compartment were consistent with locations in lymph nodes. ^{68}Ga-DOTATATE missed six liver lesions (0.75 ± 0.15 cm) which were positive on ^{18}F-FDOPA and anatomical imaging, one lung lesion which was positive on ^{18}F-FDG and anatomical imaging, and four lung lesions which were positive on ^{18}F-FDOPA and anatomical imaging studies (0.42 ± 0.11 cm). A lesion-based evaluation excluding the patients who underwent only ^{68}Ga-DOTATATE PET/CT, ^{18}F-FDG PET/CT and CT/MRI did not lead to any significant statistical change.

Besides the 450 lesions detected on ^{68}Ga-DOTATATE PET/CT and confirmed by the defined imaging comparator, 55 additional lesions were identified on ^{68}Ga-DOTATATE PET/CT that could not be confirmed by any of the other imaging studies and therefore were not included amongst the 461 lesions used in the comparator and counted as false positive (4 mediastinal lymph nodes, 11 retroperitoneal and pelvic lymph nodes, and 40 bone lesions; mean SUV_{max} 25.1 ± 34.9). On CT/MRI, 13 lesions were reported that were not positive on any functional imaging study (eight lung nodules, and five liver lesions). One abdominal lymph node and three mediastinal lymph nodes were positive only on ^{18}F-FDG PET. One bone lesion was positive only on ^{18}F-FDOPA PET/CT. ^{18}F-FDA PET/CT did not show any lesions that were not also seen on other studies.

The per-patient detection rates for ^{68}Ga-DOTATATE, ^{18}F-FDG, ^{18}F-FDOPA and ^{18}F-FDA PET/CT, and CT/MRI were 100% (22/22 patients, 95 % CI 85.1 – 100 %), 90.9 % (20/22, 95 % CI 72.2 – 97.5 %), 91.7 % (11/12, 95 % CI 64.6 – 98.5 %), 90.9 % (10/11, 95 % CI 62.3 – 98.4 %), and 100 % (22/22, 95 % CI 85.1 – 100 %), respectively. The per region detection rates for ^{68}Ga-DOTATATE, ^{18}F-FDG, ^{18}F-FDOPA and ^{18}F-FDA PET/CT, and CT/MRI were 97.0 % (identifying 65/67 involved regions, 95 % CI 89.8 – 99.2 %), 74.6 % (50/67, 95 % CI 87.7 – 99.6 %), 81.6 % (31/38, 95 % CI 66.6 – 90.8 %), 78,8 % (26/33, 95 % CI 62.3 – 89.3 %), and 83.6 % (56/67, 95 % CI 72.9 – 90.6 %), respectively. PET imaging examples comparing ^{68}Ga-DOTATATE, ^{18}F-FDG, ^{18}F-FDOPA, and ^{18}F-FDA PET/CT are shown in Figs. 1 and 2.

Discussion

We evaluated ^{68}Ga-DOTATATE PET/CT in 22 patients with sporadic metastatic PPGLs in comparison with ^{18}F-FDG, ^{18}F-FDOPA and ^{18}F-FDA PET/CT, and CT/MRI. The composite of both anatomical and all functional imaging tests was considered the imaging comparator [13, 22]. ^{68}Ga-DOTATATE PET/CT was significantly superior to all other imaging modalities in this study.

For functional imaging of metastatic PPGL, the genetic background and differentiation status of the tumor are the main factors influencing the uptake of radiopharmaceuticals [24]. ^{18}F-FDG is a sensitive but nonspecific radiopharmaceutical, which accumulates in many malignant tumors and enters cells via glucose transporters [25]. Enhanced glucose correlates with the degree of dedifferentiation, possibly caused by the shift from oxidative phosphorylation to aerobic glycolysis (Warburg effect) [26], due to upregulation of hypoxic angiogenetic pathways via hypoxia-inducible factors [27], which are mainly seen in patients with an underlying *SDHB* germline mutation. Because it has been shown to be far superior to ^{123}I-MIBG (which was not evaluated in this study) in the diagnosis of metastatic PPGLs [15, 17, 28] and its broad availability, ^{18}F-FDG PET/CT is the currently recommended functional imaging modality for diagnosing metastatic PPGL according to the Endocrine Society Clinical Practice guidelines [21]. However, the sensitivity of ^{18}F-FDG PET/CT in patients with apparently sporadic PPGL is lower than in patients with an underlying *SDHB* mutation [17, 24]. In contrast, ^{18}F-FDOPA, a highly specific radiopharmaceutical for catecholamine synthesis and targeting cells via the large amino acid transporter system [29], has shown very good results in detecting metastatic lesions in patients with sporadic PPGL [17], whereas the detection rate for metastatic lesions in *SDHB* mutation-related PPGL is poor [15, 17]. Accordingly, the guidelines of the European Association of Nuclear Medicine prefer ^{18}F-FDOPA in metastatic PPGL in the absence of an underlying *SDHB* mutation [24]. ^{18}F-FDA, which enters chromaffin cells via the norepinephrine transporter [30], has shown good detection rates for metastatic disease in patients with sporadic PPGL, whereas the reported results in *SDHB* mutation-related metastases have been less consistent [13, 15].

Given the differences in functional imaging signatures between sporadic and *SDHB* mutation-related metastatic PPGL, the reported higher expression of SSR2A and SSR3 in PPGLs with *SDH* deficiency compared to sporadic tumors [16], and the excellent performance of ^{68}Ga-DOTATATE for diagnosing *SDHB* mutation-related PPGL in our previous study [13], it was somewhat surprising that ^{68}Ga-DOTATATE performed similarly in sporadic disease. The lesions missed on ^{68}Ga-DOTATATE PET/CT were mainly located in the liver, a phenomenon that has been reported before in different NETs [31]. Kroiss et al. also demonstrated an overlap in SUVs between normal liver tissue and liver metastases of gastroenteropancreatic and non-gastroenteropancreatic NETs [32]. To avoid additional anatomical imaging, and considering the high sensitivity of MRI for liver lesions, PET/MRI might be an interesting and beneficial alternative in these patients in the future. Five lesions missed on ^{68}Ga-DOTATATE PET/CT were pulmonary lesions smaller than 0.6 cm, with four of them were positive on ^{18}F-FDOPA. Thus, dedicated MRI and CT imaging of the liver and lungs in addition to ^{68}Ga-DOTATATE PET/CT is still needed as a first line investigation in order not to miss small lung metastases as well liver metastases. ^{68}Ga-DOTATATE PET/CT can also be used to determine which patients may benefit from PRRT or from treatment with cold SSR analogs, also including patients in whom the PPGL location or extension (especially in the skull base) cannot be accessed surgically by any approach [33].

In this study, the unverifiable lesions detected only on ^{68}Ga-DOTATATE PET/CT were primarily located in the skeleton and, much less frequently, in subcentimeter mediastinal and retroperitoneal lymph nodes. Likely, more bone lesions might have been confirmed by MRI, if additional MRI scans dedicated to the spine had been performed, since this modality is very sensitive in detecting replacement of bone marrow fat and hematopoietic cells by tumor tissue [34]. Additional lesions appearing only on PET/CT with ^{68}Ga-DOTA analogs compared to any other imaging comparator have previously been reported in several studies [13, 35, 36]. Despite the high specificity of ^{68}Ga-DOTATATE for NETs [37], false-positive findings in our study population cannot be excluded given our lack of histological proof.

The current management guidelines for PPGL do not yet take PET imaging with ^{68}Ga-DOTA peptides into consideration. Yet ^{68}Ga-DOTATATE PET/CT was superior to all radiopharmaceuticals used in this study including ^{18}F-FDOPA and especially ^{18}F-FDG, suggesting that ^{68}Ga-DOTATATE has the potential to affect patient treatment plans and outcomes by identifying not only more metastatic lesions but also additional involved sites of disease as compared with all other functional imaging modalities and CT/MRI.

Our study had certain limitations, including the relatively small number of patients, although this study is the largest to date that focused on ^{68}Ga-DOTA peptide imaging in this rare disease. Furthermore, ^{18}F-FDOPA and ^{18}F-FDA PET/CT scans could only be performed in 12 and 11 patients, respectively. On the one hand, this diminishes the importance of our results regarding comparison of ^{68}Ga-DOTATATE with these radiopharmaceuticals and on the other hand, might have also influenced the results of the comparison between ^{68}Ga-DOTATATE and ^{18}F-FDG, since additional ^{18}F-FDOPA and ^{18}F-FDA scans might have led to a smaller number of false-positive lesions. Additionally, histological proof was neither feasible nor ethical for the vast majority of metastatic lesions. Although our chosen imaging comparator likely provides a close approximation of "truth", false-positive and falsenegative findings cannot be excluded. In addition, our study was biased in that we limited our lesion counts to 15 per region, thus often underestimating the number of lesions seen.

In conclusion, this study clearly demonstrated the superiority of ^{68}Ga-DOTATATE PET/CT in detection of sporadic metastatic PPGL lesions over ^{18}F-DOPA and ^{18}F-FDA PET/CT, CT/MRI, and especially ^{18}F-FDG PET/CT, which is supported by previous findings [7, 13]. Given the expected broader clinical availability of ^{68}Ga-DOTATATE along with the theranostic value of this radiopharmaceutical, a change in the clinical guidelines for functional imaging of metastatic PPGL especially from ^{18}F-FDG towards ^{68}Ga-DOTA peptides is strongly suggested. The utility of ^{68}Ga-DOTA peptides in other genotypes and nonmetastatic PPGL, or for the evaluation of treatment response, needs to be further evaluated in the future.

Acknowledgments

We acknowledge the assistance of all those who participated in this project, especially the technologists in the NIH Clinical Center PET Department.

Funding

This work was supported, in part, by the Intramural Research Program of the National Institutes of Health, Eunice Kennedy Shriver National Institute of Child Health and Human Development.

References

1. DeLellis RA. Pathology and genetics of tumours of endocrine organs. Lyon: IARC Press; 2004.
2. Martucci VL, Pacak K. Pheochromocytoma and paraganglioma: diagnosis, genetics, management, and treatment. Curr Probl Cancer. 2014;38:7–41. [PubMed: 24636754]
3. Matro J, Giubellino A, Pacak K. Current and future therapeutic approaches for metastatic pheochromocytoma and paraganglioma: focus on SDHB tumors. Horm Metab Res. 2013;45:147–53. [PubMed: 23322515]
4. Turkova H, Prodanov T, Maly M, Martucci V, Adams K, Widimsky J Jr, et al. Characteristics and outcomes of metastatic SDHB and sporadic pheochromocytoma/paraganglioma: a National Institutes of Health study. Endocr Pract. 2016;22:302–14. [PubMed: 26523625]
5. Reubi JC, Waser B, Schaer JC, Laissue JA. Somatostatin receptor sst1-sst5 expression in normal and neoplastic human tissues using receptor autoradiography with subtype-selective ligands. Eur J Nucl Med. 2001;28:836–46. [PubMed: 11504080]
6. Sadowski SM, Millo C, Cottle-Delisle C, Merkel R, Yang LA, Herscovitch P, et al. Results of (68)gallium-DOTATATE PET/CT scanning in patients with multiple endocrine neoplasia type 1. J Am Coll Surg. 2015;221:509–17. [PubMed: 26206648]
7. Tan TH, Hussein Z, Saad FF, Shuaib IL. Diagnostic performance of (68)Ga-DOTATATE PET/CT, (18)F-FDG PET/CT and (131)I-MIBG scintigraphy in mapping metastatic pheochromocytoma and paraganglioma. Nucl Med Mol Imaging. 2015;49:143–51. [PubMed: 26085860]
8. Naji M, Zhao C, Welsh SJ, Meades R, Win Z, Ferrarese A, et al. 68Ga-DOTA-TATE PET vs. 123I-MIBG in identifying malignant neural crest tumours. Mol Imaging Biol. 2011;13:769–75. [PubMed: 20700766]
9. Win Z, Al-Nahhas A, Towey D, Todd JF, Rubello D, Lewington V, et al. 68Ga-DOTATATE PET in neuroectodermal tumours: first experience. Nucl Med Commun. 2007;28:359–63. [PubMed: 17414885]
10. Sharma P, Thakar A, Suman KC, Dhull VS, Singh H, Naswa N, et al. 68Ga-DOTANOC PET/CT for baseline evaluation of patients with head and neck paraganglioma. J Nucl Med. 2013;54:841–7. [PubMed: 23520216]
11. Naswa N, Sharma P, Nazar AH, Agarwal KK, Kumar R, Ammini AC, et al. Prospective evaluation of 68Ga-DOTA-NOC PET-CT in phaeochromocytoma and paraganglioma: preliminary results from a single centre study. Eur Radiol. 2012;22:710–9. [PubMed: 21971823]
12. Puranik AD, Kulkarni HR, Singh A, Baum RP. Peptide receptor radionuclide therapy with (90)Y/(177)Lu-labelled peptides for in-operable head and neck paragangliomas (glomus tumours). Eur J Nucl Med Mol Imaging. 2015;42:1223–30. [PubMed: 25822655]
13. Janssen I, Blanchet EM, Adams K, Chen CC, Millo CM, Herscovitch P, et al. Superiority of [68Ga]-DOTATATE PET/CT to other functional imaging modalities in the localization of SDHB-associated metastatic pheochromocytoma and paraganglioma. Clin Cancer Res. 2015;21:3888–95. [PubMed: 25873086]
14. Taieb D, Neumann H, Rubello D, Al-Nahhas A, Guillet B, Hindie E. Modern nuclear imaging for paragangliomas: beyond SPECT. J Nucl Med. 2012;53:264–74. [PubMed: 22302963]
15. Timmers HJ, Kozupa A, Chen CC, Carrasquillo JA, Ling A, Eisenhofer G, et al. Superiority of fluorodeoxyglucose positron emission tomography to other functional imaging techniques in the evaluation of metastatic SDHB-associated pheochromocytoma and paraganglioma. J Clin Oncol. 2007;25:2262–9. [PubMed: 17538171]

16. Elston MS, Meyer-Rochow GY, Conaglen HM, Clarkson A, Clifton-Bligh RJ, Conaglen JV, et al. Increased SSTR2A and SSTR3 expression in succinate dehydrogenase-deficient pheochromocytomas and paragangliomas. Hum Pathol. 2015;46:390–6. [PubMed: 25554089]
17. Timmers HJ, Chen CC, Carrasquillo JA, Whatley M, Ling A, Havekes B, et al. Comparison of 18F-fluoro-L-DOPA, 18F-fluoro-deoxyglucose, and 18F-fluorodopamine PET and 123I-MIBG scintigraphy in the localization of pheochromocytoma and paraganglioma. J Clin Endocrinol Metab. 2009;94:4757–67. [PubMed: 19864450]
18. Fonte JS, Robles JF, Chen CC, Reynolds J, Whatley M, Ling A, et al. False-negative 123I-MIBG SPECT is most commonly found in SDHB-related pheochromocytoma or paraganglioma with high frequency to develop metastatic disease. Endocr Relat Cancer. 2012;19:83–93. [PubMed: 22167067]
19. Loh KC, Fitzgerald PA, Matthay KK, Yeo PP, Price DC. The treatment of malignant pheochromocytoma with iodine-131 metaiodobenzylguanidine (131I-MIBG): a comprehensive review of 116 reported patients. J Endocrinol Invest. 1997;20:648–58. [PubMed: 9492103]
20. Niemeijer ND, Alblas G, van Hulsteijn LT, Dekkers OM, Corssmit EP. Chemotherapy with cyclophosphamide, vincristine and dacarbazine for malignant paraganglioma and pheochromocytoma: systematic review and meta-analysis. Clin Endocrinol (Oxf). 2014;81:642–51. [PubMed: 25041164]
21. Lenders JW, Duh QY, Eisenhofer G, Gimenez-Roqueplo AP, Grebe SK, Murad MH, et al. Pheochromocytoma and paraganglioma: an Endocrine Society clinical practice guideline. J Clin Endocrinol Metab. 2014;99:1915–42. [PubMed: 24893135]
22. Hofman MS, Hicks RJ. Moving beyond “lumpology”: PET/CT imaging of pheochromocytoma and paraganglioma. Clin Cancer Res. 2015;21:3815–7. [PubMed: 26152741]
23. Timmers HJ, Hadi M, Carrasquillo JA, Chen CC, Martiniova L, Whatley M, et al. The effects of carbidopa on uptake of 6-18F-fluoro-L-DOPA in PET of pheochromocytoma and extraadrenal abdominal paraganglioma. J Nucl Med. 2007;48:1599–606. [PubMed: 17873132]
24. Taieb D, Timmers HJ, Hindie E, Guillet BA, Neumann HP, Walz MK, et al. EANM 2012 guidelines for radionuclide imaging of phaeochromocytoma and paraganglioma. Eur J Nucl Med Mol Imaging. 2012;39:1977–95. [PubMed: 22926712]
25. Belhocine T, Spaepen K, Dusart M, Castaigne C, Muylle K, Bourgeois P, et al. 18FDG PET in oncology: the best and the worst. Int J Oncol. 2006;28:1249–61. [PubMed: 16596242]
26. Warburg O On the origin of cancer cells. Science. 1956;123:309–14. [PubMed: 13298683]
27. Jochmanova I, Yang C, Zhuang Z, Pacak K. Hypoxia-inducible factor signaling in pheochromocytoma: turning the rudder in the right direction. J Natl Cancer Inst. 2013;105:1270–83. [PubMed: 23940289]
28. Timmers HJ, Chen CC, Carrasquillo JA, Whatley M, Ling A, Eisenhofer G, et al. Staging and functional characterization of pheochromocytoma and paraganglioma by 18F-fluorodeoxyglucose (18F-FDG) positron emission tomography. J Natl Cancer Inst. 2012;104:700–8. [PubMed: 22517990]
29. Havekes B, King K, Lai EW, Romijn JA, Corssmit EP, Pacak K. New imaging approaches to phaeochromocytomas and paragangliomas. Clin Endocrinol (Oxf). 2010;72:137–45. [PubMed: 19508681]
30. Timmers HJ, Eisenhofer G, Carrasquillo JA, Chen CC, Whatley M, Ling A, et al. Use of 6-[18F]-fluorodopamine positron emission tomography (PET) as first-line investigation for the diagnosis and localization of non-metastatic and metastatic phaeochromocytoma (PHEO). Clin Endocrinol (Oxf). 2009;71:11–7. [PubMed: 19138315]
31. Sounness BD, Schembri GP. 68Ga-Dotatate avid medullary thyroid cancer with occult liver metastases. Clin Nucl Med. 2014;39:87–90. [PubMed: 24097007]
32. Kroiss A, Putzer D, Decristoforo C, Uprimny C, Warwitz B, Nilica B, et al. 68Ga-DOTA-TOC uptake in neuroendocrine tumour and healthy tissue: differentiation of physiological uptake and pathological processes in PET/CT. Eur J Nucl Med Mol Imaging. 2013;40:514–23. [PubMed: 23291643]

33. van Hulsteijn LT, van Duinen N, Verbist BM, Jansen JC, van der Klaauw AA, Smit JW, et al. Effects of octreotide therapy in progressive head and neck paragangliomas: case series. Head Neck. 2013;35:E391–6. [PubMed: 23606330]
34. Lecouvet FE, Talbot JN, Messiou C, Bourguet P, Liu Y, de Souza NM. Monitoring the response of bone metastases to treatment with magnetic resonance imaging and nuclear medicine techniques: a review and position statement by the European Organisation for Research and Treatment of Cancer Imaging Group. Eur J Cancer. 2014;50:2519–31. [PubMed: 25139492]
35. Hofman MS, Kong G, Neels OC, Eu P, Hong E, Hicks RJ. High management impact of Ga-68 DOTATATE (GaTate) PET/CT for imaging neuroendocrine and other somatostatin expressing tumours. J Med Imaging Radiat Oncol. 2012;56:40–7. [PubMed: 22339744]
36. Maurice JB, Troke R, Win Z, Ramachandran R, Al-Nahhas A, Naji M, et al. A comparison of the performance of 68Ga-DOTATATE PET/CT and 123I-MIBG SPECT in the diagnosis and follow-up of phaeochromocytoma and paraganglioma. Eur J Nucl Med Mol Imaging. 2012;39:1266–70. [PubMed: 22526961]
37. Yang J, Kan Y, Ge BH, Yuan L, Li C, Zhao W. Diagnostic role of gallium-68 DOTATOC and gallium-68 DOTATATE PET in patients with neuroendocrine tumors: a meta-analysis. Acta Radiol. 2014;55:389–98. [PubMed: 23928010]

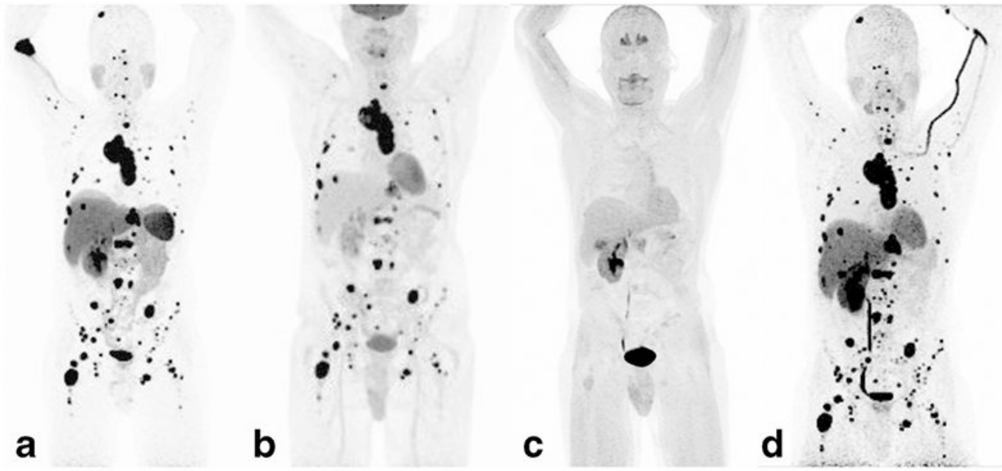

Fig. 1.

A 39-year-old man with sporadic metastatic paraganglioma, who was first diagnosed with a 9.5-cm paraganglioma involving the left kidney, and bone metastases in 2014. The ^{68}Ga-DOTATATE (**a**), ^{18}F-FDG (**b**), and ^{18}F-FDA (**d**) PET images show very similar extensive metastatic disease involving bone, liver, and mediastinal and retroperitoneal lymph nodes. The ^{18}F-FDOPA PET image (**c**) is almost negative

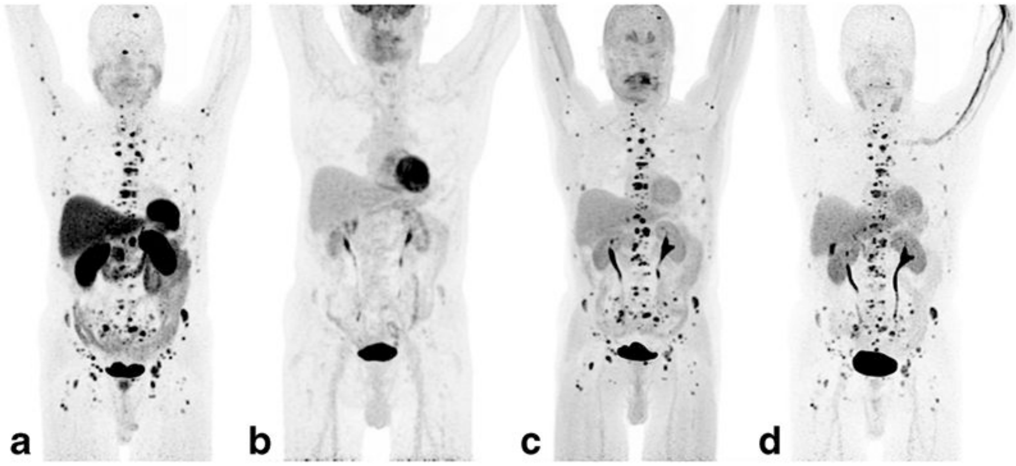

Fig. 2.

A 64-year-old man with sporadic metastatic paraganglioma, who was first diagnosed with a right adrenal pheochromocytoma in 1994 and metastatic disease to the bones in 2009. The ^{68}Ga-DOTATATE (**a**), ^{18}F-FDOPA (**c**), and ^{18}F-FDA (**d**) PET images show very similar extensive metastatic bone disease. The ^{18}F-FDG PET image (**b**) is almost negative

Table 1

Patient characteristics

Patient no.	Sex	Tested negative	Age (years)		Location of primary	Hypersecretion	Time to metastasis (years)	Location of metastases
			Diagnosis	Time of study				
1	m	*SDHx, VHL*	61	75	Right adrenal	NM, NE, DA, CgA	12	A/P
2	f	*SDHx*	52	55	Left adrenal	NM, NE, CgA	3	A/P, B
3	f	*SDHx*	54	54	Left para-adrenal	NM, NE, CgA	0	A/P, B
4	m	*SDHx, MEN, VHL, TMEM 127*	20	37	Right para-adrenal	NM	0	A/P, B, Li, Lu
5	m	*SDHx, MEN, VHL*	27	30	Unknown	NE, NM, DA, CgA	0	A/P, B, Li, Me
6	f	*SDHx*	21	46	Right glomus jugulare	None	9	A/P, B, Me, Ne
7	f	*SDHx, MEN, VHL, MAX, TMEM 127*	52	64	Left adrenal	NM, NE, DA, MTT, CgA	6	A/P, B, Li, Lu
8	f	*SDHx, MAX*	38	47	Left adrenal	NM, MN, CgA	7	B
9	f	*SDHx*	12	31	Left para-adrenal	CgA,	4	A/P, B, Lu
10	m	*SDHx*	56	59	Right adrenal	NM, MN, NE, DA, CgA	0	A/P, B, Lu, Ne
11	m	*SDHx*	42	52	Unknown	DA, CgA, MTT	5	A/P, B, Lu, Me, Ne
12	m	*SDHx*	49	52	Right retroperitoneal	CgA	0	B, Li
13	m	*SDHx, VHL*	54	61	Left adrenal	NM, NE, CgA, DA	0	A/P, B, Li, Lu, Me
14	m	*SDHx, MAX*	70	73	Left adrenal	NM, NE, CgA, DA	0	A/P, Lu, Me
15	m	*SDHx*	34	35	Left retroperitoneal	NM, NE, MN, Epi, DA, CgA	0	A/P, B, Li, Lu
16	m	*SDHx*	31	43	Right adrenal	NM, NE, DA, CgA	6	A/P, B, Me
17	m	*SDHx, VHL*	23	25	Right adrenal	NM, NE, DA, CgA, MTT	0	A/P, B, Li, Lu
18	m	*SDHx*	38	39	Right para-adrenal	NM, CgA	0	A/P, B, Li, Me
19	m	*SDHx*	43	64	Right adrenal	NM, NE, MN, Epi, DA, CgA, MTT	15	A/P, B
20	m	*SDHx*	34	41	Left adrenal	MTT	5	A/P, B
21	f	*SDHx*	63	64	Left adrenal	NM, NE, Epi, CgA, MTT	0	B, Li
22	m	*SDHx*	37	39	Right adrenal	NM, DA	2	B, Li, Lu

A/P abdominal/pelvic compartment, *B* bones, *CgA* chromogranin A, *DA* dopamine, *Epi* epinephrine, *Li* liver, *Lu* lungs, *m* male, *MAX* myc-associated factor X, *Me* mediastinum, *MTT* methoxytyramine, *Ne* neck, *NE* norepinephrine, *NM* normetanephrine, *TMEM 127* trans-membrane protein 127

Table 2

Numbers of lesions identified on ^{68}Ga-DOTATATE, ^{18}F-FDG, ^{18}F-FDOPA and ^{18}F-FDA PET/CT, and CT/MRI compared to lesions identified by the imaging comparator

Lesion location	^{68}Ga-DOTATATE PET/CT	^{18}F-FDG PET/CT	^{18}F-FDOPA PET/CT[a]	^{18}F-FDA PET/CT[a]	CT/MRI
All compartments	450/461	226/461	181/242	160/206	376/461
Mediastinum	46/46	26/46	17/24	21/21	27/46
Lungs	89/94	52/94	52/53	26/38	89/94
Abdomen	74/74	42/74	30/41	35/38	57/74
Liver	42/48	6/48	11/13	9/13	45/48
Bone	199/199	100/199	71/111	69/96	158/199

[a]Not all patients underwent PET/CT scans with these radiopharmaceuticals

Table 3

Lesion detection rates for ^{68}Ga-DOTATATE, ^{18}F-FDG, ^{18}F-FDOPA and ^{18}F-FDA PET/CT, and CT/MRI

Lesion location	^{68}Ga-DOTATATE PET/CT		^{18}F-FDG PET/CT		^{18}F-FDOPA PET/CT		^{18}F-FDA PET/CT		CT/MRI	
	Detection rate (%)	95 % CI (%)	Detection rate (%)	95 % CI (%)	Detection rate (%)	95 % CI (%)	Detection rate (%)	95 % CI (%)	Detection rate (%)	95 % CI (%)
All compartments	97.6	95.8 – 98.7	49.2	44.5 – 53.6	74.8	69.0 – 79.9	77.7	71.5 – 82.8	81.6	77.8 – 84.8
Mediastinum	100	92.3 – 100	56.5	42.3 – 69.8	70.8	50.8 – 85.1	100	84.5 – 100	58.7	44.3 – 71.7
Lungs	94.7	95.1 – 97.1	55.3	45.3 – 65.0	98.1	90.1 – 99.7	68.4	52.5 – 80.9	94.7	88.2 – 97.7
Abdomen	100	95.1 – 100	56.8	45.3.4 – 67.4	73.2	58.1 – 84.3	92.1	79.2 – 97.3	77.0	66.3 – 85.1
Liver	87.5	75.3 – 94.1	12.5	5.9 – 24.7	84.5	57.8 – 95.7	69.2	42.4 – 87.3	93.8	83.2 – 97.8
Bone	100	98.1 – 100	50.3	43.4 – 57.1	64.0	54.7 – 72.3	71.2	62.2 – 79.9	79.4	73.3 – 84.4